462 J. THERMOPHYSICS VOL. 4, NO. 4

High-Temperature Thermal Diffusivity Determination Procedure for Solids and Liquids

Yildiz Bayazitoglu,* P. V. R. Suryanarayana,† and Udaya B. Sathuvalli‡
Rice University, Houston, Texas 77251

A new method for measuring the thermal diffusivity of materials at high temperatures is presented. The method is applicable to solids on Earth and liquids in the reduced gravity environment of space. It is especially suited to levitated liquid metals at elevated temperatures, where thermal diffusivity data are not available. The method is applied in two parts, such that lumped analysis is valid in the first part, and Fourier's law of conduction in the second. In both parts, the spherical specimen is assumed to have been heated to a desired temperature and cooled. An inverse conduction problem is then formulated and solved using Laplace transformation techniques. Using this solution, the sample sizes, and experimentally obtained surface temperature history, the thermal diffusivity is determined by minimizing a function that satisfies the heat balance at the surface. Minimization is performed using a modified quasilinearization algorithm. The method is demonstrated using theoretical cooling curves for three materials—nickel, niobium, and palladium (for $Nr = 4$ and 10)—and is shown to be accurate. Accuracy is very sensitive to error in the temperature data and increases with better curve fits to the temperature data. An error analysis is also performed, and the effect of errors in the various parameters on the evaluated thermal diffusivity is determined. An experimental study for solids on Earth is suggested before development for implementation in space.

Nomenclature

a_l, $l = 0..N$ = coefficients of Nth degree polynomial fit
a = characteristic size of specimen
Bi = Biot number, $\epsilon\bar{\sigma}T_i^3R/\kappa$
C_p = specific heat of specimen, J/kgK
c_1,c_2 = coefficients of the exponential fit
F = shape factor between sphere and surrounding walls
M = radiation to heat capacity ratio, $\epsilon F/\rho C_p$
Ma = Marangoni number, $-\mathrm{d}\gamma/\mathrm{d}T \Delta T\, d/\rho\nu\kappa$
Nr = conduction-to-radiation parameter, $\kappa/\epsilon\bar{\sigma}T_i^3R$
R = equilibrium radius of sphere, m
r = radius
$\bar{r}$ = nondimensional radius, r/R
T = temperature
t = time
α = thermal diffusivity of specimen, m^2/s
γ = surface tension, N/m
$\mathrm{d}\gamma/\mathrm{d}T$ = temperature gradient of surface tension, -10^{-4}N/mK
ϵ = total hemispherical emissivity of surface
Θ = nondimensional temperature, T/T_i
κ = thermal conductivity of specimen, W/m^2
ν = kinematic viscosity of specimen, m^2/s
ρ = density of specimen, kg/m^3
$\bar{\sigma}$ = Stefan-Boltzmann constant
τ = nondimensional time, $\alpha t/R^2$

Subscripts

1 = small specimen experiment parameter
2 = large specimen experiment parameter
$i1$ = initial parameter, small-droplet experiment
$i2$ = initial parameter, large-droplet experiment
s = surface parameter
∞ = ambient parameter

Introduction

THERMAL diffusivity is an important material property that governs the rate of heat propagation in transient processes and is defined as

$$\alpha = \kappa/(\rho C_p) \tag{1}$$

where, in the case of anisotropic inhomogeneous media, κ and α are tensors. Thermal diffusivity has been the concern of engineers and physicists for over a century. In addition to being a material property of considerable importance, measurement of thermal diffusivity is often the starting point in the measurement of thermal conductivity. A large amount of data is available on thermal conductivity and thermal diffusivity of solids[1] over a wide range of temperatures. Although a high degree of sophistication has been achieved in the measurement of solid thermal diffusivities, there is, at best, a scant availability of data on the thermal diffusivity of liquids, especially at high temperatures. Often, extrapolation from a few solid-phase data points is the only recourse. There are various reasons for the difficulty in measuring thermal diffusivities of high-temperature liquids. Some of these are summarized below.

1) The geometry of the sample is complicated, due to the necessity of a container for the liquid.

2) Most materials at high temperatures are highly corrosive and present the problem of crucible contamination and chemical reactions, which have to be eliminated.

3) Devices to prevent convection within the sample are necessary.

4) Mechanical problems limit the ability to maintain the liquid in shapes that ensure one-dimensional conduction, with all other forms of heat transfer eliminated.

5) Evaporation and vapor bubble formation will bias the measurements.

Many of the methods used to measure liquid thermal diffusivities, such as transient hot-wire methods,[2,3] flash heating methods,[4] etc., are essentially extensions or improvements over methods used for solids. Over the past few years, Cezairliyan[5] and associates have developed a dynamic method for measuring various high-temperature thermophysical properties of liquids. Although this method has not yet been applied to thermal diffusivity measurements per se, Cezairliyan notes in his paper that this can be done. Araki[6] and Araki and

---

Received May 26, 1989; revision received Aug. 24, 1989.

[*] Professor, Mechanical Engineering and Materials Science Department. Member AIAA.

[†] Graduate Student, Mechanical Engineering and Materials Science Department. Student Member AIAA.

[‡] Graduate Student, Mechanical Engineering and Materials Science Department.

Natsui[7] have described a stepwise heating method for measuring the thermal diffusivity of liquids with a high accuracy.

However, all these methods are limited by the fact that contact with a solid, whose melting point is greater than the temperature at which the liquid is being studied, is necessary. Such a situation is unacceptable in the case of liquid metals, which are highly reactive at temperatures beyond 2000 K. At present, there is a paucity of information on thermal diffusivity of liquid metals and other high-temperature corrosive melts. Such information is of great importance in many spheres of engineering and materials science and cannot be over-emphasized. Thus, there is a strong necessity to obtain thermal diffusivity data beyond the 2000 K mark, which has been crossed only on occasion.

We present here a new method for measuring the thermal diffusivity of materials at high temperatures. Using an appropriate levitation technique, a very small sample is levitated and heated. The temperature at its surface is measured at various instants of time. Next, a sphere of a larger radius is levitated in the same apparatus, and, as in the previous case, its surface temperature history is obtained. The experiment is carried out in two parts to eliminate the need to know other thermophysical properties. In both cases, the levitated sample is heated until equilibrium and allowed to cool by turning off the heating apparatus. The size of the specimen is chosen such that lumped analysis is valid within the sphere in the first case, and Fourier's law in the second case. An inverse conduction problem is then formulated and solved using a method outlined in this work. (An inverse problem in heat conduction has additional boundary conditions, the surface conditions or a property being unknown. Beck et al.[8] provide an extensive discussion of this variety of problem.) Using this solution, and the experimental data, the thermal diffusivity is determined. The only experimental data necessary are the radius of the sample and the surface temperature history in both cases. In the case of liquid samples, such data are to be obtained in a reduced gravity environment. In most levitation systems designed with space-based application in mind, such data are obtained routinely as part of other more elaborate studies (such as solidification, subcooling, etc.). Thus, an advantage of this method is that no new equipment or data-gathering requirements are imposed on an existing levitation system. Moreover, the method is equally applicable for solids, as long as they are spherical in shape. The method is demonstrated for three cases: nickel, niobium, and palladium; and representative results are obtained in all three cases. An error analysis is also performed, and the effect of errors in the various parameters on the evaluated thermal diffusivity is determined.

Theory of Measurement

The availability of levitation techniques has made it possible to study uncontaminated liquid metals and alloys several hundred degrees beyond their melting points. Many levitation methods have been developed under the class of "containerless processing techniques," especially with reference to their application in the reduced gravity environment of space. A good discussion of containerless processing technologies is given by Barmatz.[9] Of these methods, two better suited for the purpose of this work are described below.

When a metal specimen is placed in a time-varying electromagnetic field, it is subjected to Lorentz forces and ohmic heating due to the induced currents. When these are of a sufficient magnitude, the metal may be levitated and melted. In microgravity applications, the fields are orders of magnitude lower than on Earth. Therefore, induction heating may be insufficient and may have to be supplemented/replaced by additional heating coils or resistive heaters. In a typical electromagnetic levitation apparatus (Fig. 1), two oppositely wound coils are supplied with a high-frequency alternating current, and the specimen introduced into the coils. The whole apparatus is enclosed in a chamber filled with an inert gas. The molten levitated metal allows examination and processing of an uncontaminated, container-free material in its liquid state. The size of the specimen is limited by the inner coil diameter, sample conductivity, available frequency and current density of the field. Electromagnetic levitation has already been used in measuring various liquid metal properties at high temperatures, such as heat capacities, heats of fusion, surface tension, and emissivity. It is also of current interest as a viable space manufacturing method in the future space station projects.

Alternately, an acoustic levitation technique may be employed. A typical acoustic levitator (Fig. 2) has an acoustic horn that produces an ultrasonic acoustic wave. On reflection by a suitably designed and placed reflector, a standing wave is created in the chamber. The specimen levitates at the nodes. For high-temperature applications, a separate heater (such as a radiative resistance heater) is necessary. The size of the specimen is restricted by its density and by the acoustic radiation pressure on the surface. However, due to the larger melting times, higher force requirements, and instability of high-temperature acoustic levitation, it has not been used extensively for liquid metals.

Irrespective of the actual method employed, it becomes possible to obtain a spherical liquid droplet, free of container contamination, and exposed to the radiatively cooling environment of space. At time $t > 0$, the levitated sphere of equilibrium radius R_2 is subjected to cooling by the environment by turning off the heating coils or resistors. The temperature at the surface of the sphere is monitored as a function of time, using a suitable measurement method (for example, an ellipsometric method[10]). For a liquid in the presence of gravity, the equilibrium shape deviates from the spherical, but in microgravity, the shape is almost entirely spherical. The problem for $t > 0$ is governed by

$$\frac{1}{r^2}\frac{\partial}{\partial r}\left(r^2\frac{\partial T}{\partial r}\right)=\frac{1}{\alpha}\frac{\partial T}{\partial t}, \qquad 0 < r \leq R \tag{2}$$

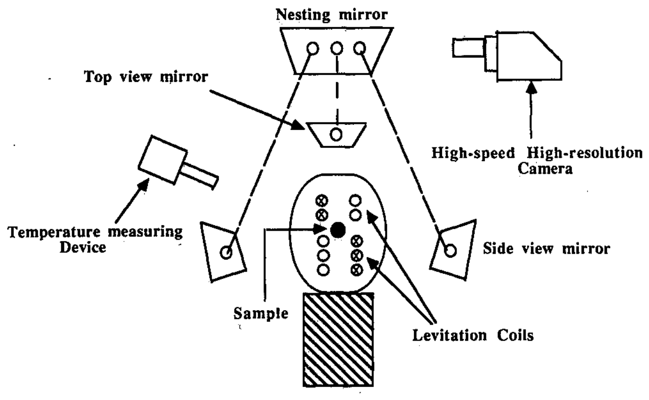

Fig. 1 Typical electromagnetic levitator.

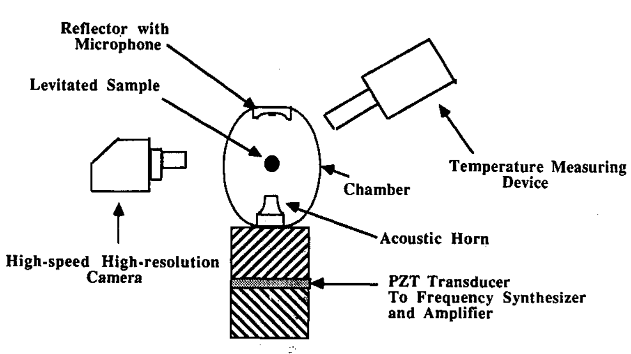

Fig. 2 Typical acoustic levitator.

subjected to

$$\frac{\partial T}{\partial r}=0, \qquad \text{at } r=0, \qquad t>0 \tag{3a}$$

$$-\kappa\frac{\partial T}{\partial r}=q_l, \qquad \text{at } r=R, \qquad t>0 \tag{3b}$$

and the initial condition

$$T(t=0,\, r)=T_i \tag{3c}$$

In Eq. (3b), q_l is the net heat loss per unit area from the surface. If the droplet is suspended in vacuum, conduction in the outer medium is absent, and we have

$$q_l=\epsilon\bar{\sigma}F(T_s^4-T_\infty^4) \tag{4}$$

Here, F is the shape factor. For a sphere within an enclosure, it is equal to unity. In the presence of a surrounding medium (such as inert gas, vapor, or boiling impurities), conduction may still be assumed negligible in the outer medium, since its thermal conductivity is very low in comparison to that of the droplet. However, due to the high temperatures, the participation of the surrounding medium in the radiation transfer must be considered. Bayazitoglu and Suryanarayana[11,12] have studied the effect of the participating medium in such a problem and have presented expressions for the effective emissivity of the droplet as a result of the presence of a participating medium. By using these values for the effective emissivity in place of ϵ in Eq. (4), the effect of a participating medium can be accounted for in this work.

Equation (2) is the starting point for thermal diffusivity measurements. In using this formulation to measure α, one requires, in addition to the temperature of the surface as a function of time, the emissivity of the surface and the heat capacity of the material being studied. In addition, it is possible that due to the presence of other surfaces at different temperatures, F may not be equal to unity and may have to be known a priori. Therefore, in order to eliminate the necessity for a knowledge of material properties, and to account for bulk radiation effects, the following comparative method, which is composed of two experimental phases, is proposed. Both experiments are conducted within the same experimental set-up, with the only change being in the size of the levitated droplet.

Small-Droplet Experiment

When the Biot number is small (i.e., less than 0.1), the thermal conductance is of the material is considerable compared to that of the surface and lumped analysis is valid. Hence, for small spheres of high thermal conductivity, lumped analysis is valid, and the following equation governs the heat transfer from the sphere:

$$\rho\, C_pV\frac{dT}{dt}=-\epsilon\bar{\sigma}FA_s[T_s(t)^4-T_\infty{}^4] \tag{5}$$

with the initial condition of Eq. (3c). Here, V and A_s are the volume and surface area of the specimen, respectively. In general, $\rho\, C_p$ and ϵ are functions of temperature. For a sphere, rearrangement of Eq. (5) gives

$$\frac{dT_s}{dt}+\frac{3\bar{\sigma}M}{R_1}(T_s^4-T_\infty^4)=0 \tag{6a}$$

with the initial condition

$$T_s(t=0)=T_{i1} \tag{6b}$$

Here,

$$M=\frac{\epsilon F}{\rho C_p} \tag{7}$$

For lumped analysis to be valid, the Biot number

$$Bi=(\epsilon\bar{\sigma}T_i^3R_1)/\kappa \tag{8}$$

must be less than 0.1. It must be noted that the Biot number, as defined by Eq. (8), is nothing but the reciprocal of the conduction-to-radiation parameter Nr. The droplet size requirements as a result of this restriction are discussed in the results and discussion section.

If the droplet size and the surface temperature as a function of time are known, M can be determined from Eq. (6a) directly by integration. The evaluated M is then used in the large droplet test.

There is one rather fortunate byproduct of the small droplet experiment. As mentioned earlier, some data are already available on the heat capacities of high-temperature materials.[13] Thus, by simple modification of the experimental apparatus and a calculation of the radiation shape factor F, the total hemispherical emissivity ϵ of the material being studied may also be determined from a measurement of M.

Large-Droplet Experiment

A large droplet is now levitated, so that the system of Eqs. (4) and (2) are valid. The boundary condition of Eq. (3b) can be modified to give

$$\frac{\partial T}{\partial r}=-\frac{M\bar{\sigma}}{\alpha}[T_s^4-T_\infty^4], \qquad \text{at } r=R_2 \tag{9}$$

The size of the droplet in this phase must be such that $Bi \geq 0.1$.

Thus, from the small-droplet experiment, M is determined, and used when the boundary condition of Eq. (9) is imposed. It is now left to describe a method to determine α from the large-droplet experiment, using the experimentally obtained surface temperature history. This is undertaken in the next section.

Solution Method

Without loss of generality, we assume that $T_\infty=0$ in all cases. Then, from the small-droplet experiment, integration of Eq. (6a) with $T_\infty=0$, gives

$$M=\frac{R_1}{9\bar{\sigma}t}\left[\frac{1}{T^3}-\frac{1}{T_{i1}^3}\right] \tag{10}$$

Once R_1 and T at any time t are known, M, a constant for any given material, can be determined from Eq. (10). Since the surface temperature history of the small droplet is available, M can be determined at all the time steps and averaged to reduce the error. Alternately, M can be found to be the value that minimizes the error between the theoretically obtained and experimentally measured values of the surface temperatures. Finding M is the sole purpose of the small-droplet experiment and we now proceed to the large-droplet experiment.

For one-dimensional conduction, using the nondimensional scheme indicated in the nomenclature, Eq. (2), the governing equation, and Eqs. (3a), (3b), and (9) reduce to

$$\frac{\partial^2\Theta}{\partial\bar{r}^2}+\frac{2}{\bar{r}}\frac{\partial\Theta}{\partial\bar{r}}=\frac{\partial\Theta}{\partial\tau} \tag{11}$$

subject to

$$\frac{\partial\Theta}{\partial\bar{r}}=0, \qquad \text{at } \bar{r}=0, \qquad \tau>0 \tag{12a}$$

$$-\frac{\partial\Theta}{\partial\bar{r}}=\frac{1}{Nr}\Theta^4, \qquad \text{at } \bar{r}=1, \qquad \tau>0 \tag{12b}$$

and the initial condition

$$\Theta(\bar{r}, \tau=0)=1 \tag{12c}$$

Equation (11), subjected to the boundary conditions of Eqs. (12), cannot be solved analytically, owing to the nonlinearity of the heat balance boundary condition of Eq. (12b). Therefore, using the experimentally obtained surface temperature history, an inverse conduction problem is posed for the larger sphere. (The satisfaction of the heat flux boundary condition is later used as a criterion to find α.) Thus, the problem reduces to solving Eq. (11), subject to Eqs. (12a) and (12b), and the known surface temperature as a function of time,

$$\Theta=g(\tau), \qquad \text{at } \bar{r}=1 \tag{13}$$

The function $g(\tau)$ is obtained by using a suitable curve fit on the discrete set of temperature data points obtained experimentally. In general,

$$g(\tau)=\sum_{l=0}^{N} a_l \tau^1 + c_1 e^{c_2\tau} \tag{14}$$

Equation (14) incorporates polynomial and exponential terms to enable suitable curve fitting, as desired by the experimenter.

In solving this system of equations, the following simplifying assumptions have been made: 1) one-dimensional conduction prevails in the sphere (valid for solids, and for liquids in microgravity); 2) radiation is the only form of heat loss from the surface of the sphere; and, finally, 3) the α is constant within the temperature range of the experiment.

Applying the Laplace transformation to Eq. (11), subject to the initial condition of Eq. (12c), gives

$$\frac{d^2(\bar{r}\bar{\Theta})}{d\bar{r}^2}-p^2(\bar{r}\bar{\Theta})=-1 \tag{15}$$

where $p2=s$, and $\bar{\Theta}(\bar{r},s)$ is the Laplace transform of $\Theta(\bar{r},\tau)$ and given by

$$\Theta(\bar{r},s)=\int_0^{\infty} e^{-s\tau}\Theta(\bar{r},\tau)\,d\tau, \qquad \tau>0 \tag{16}$$

where s is the Laplace transform variable. The boundary condition of Eq. (12a) simply implies that $\bar{\Theta}(\bar{r},\tau)$, and hence $\bar{\Theta}(\bar{r},s)$ be bounded at the origin. Laplace transformation of the surface temperature boundary condition of Eq. (14) results in

$$G(s)=\sum_{l=0}^{N} l!\frac{a_l}{s^{l+1}}+\frac{C_1}{s-c_2} \tag{17}$$

Integrating Eq. (15) and applying the boundary conditions, one obtains

$$\bar{\Theta}(\bar{r},s)=\frac{1}{s}-\frac{1}{\bar{r}}\frac{\sinh(p\bar{r})}{\sinh(p)}+G(s)\frac{\sinh(p\bar{r})}{\bar{r}\sinh(p)} \tag{18}$$

where $p=\sqrt{s}$. The temperature $\bar{\Theta}(\bar{r},\tau)$ is the inverse Laplace transform of Eq. (18),

$$\bar{\Theta}(\bar{r},\tau)=L^{-1}[\bar{\Theta}(\bar{r},s)]$$

Since $\bar{\Theta}(\bar{r},s)$ is a single-valued function, the inverse Laplace transform in the Eq. (18) is obtained using Cauchy's residue theorem. Then, $\Theta(\bar{r},\tau)$ is given by

$$\begin{aligned}\bar{\Theta}(\bar{r},\tau)={}&\sum_{l=0}^{N} a_l\tau^l+\frac{(a_0-1)}{\bar{r}}\sum_{n=1}^{\infty}\frac{2(-1)^n\sin(\omega\bar{r})e^{-b\tau}}{\omega}\\&+\sum_{l=1}^{N}\frac{l!a_l}{\bar{r}}\sum_{n=1}^{\infty}\frac{2(-1)^{n+1}\sin(\omega\bar{r})}{b^l\omega}\left[e^{-b\tau}+\sum_{m=0}^{l-1}\frac{(b\tau)^m(-1)^{m+1}}{m!}\right]\\&+\frac{c_1}{\bar{r}}\left[\frac{\sinh(\sqrt{c_2}\bar{r})}{\sinh(\sqrt{c_2})}+\sum_{n=1}^{\infty}\frac{2\omega(-1)^n e^{-c_2\tau}\sinh(\omega\bar{r})}{(c_2+\omega^2)}\right]\end{aligned} \tag{19}$$

where $b=n^2\pi^2$, $\omega=n\,\pi$, and N is the degree of the curve fit chosen to represent the surface temperature history.

It now remains to find α. The surface heat balance condition (Eq. 12b) has to be satisfied at all times. This condition can now be employed to find α. Eq. (12b) implies that

$$\Phi=\sum_{i=1}^{k}\left[\frac{\partial\Theta}{\partial\bar{r}}+\frac{1}{Nr}\Theta^4\right]_i^2=0, \qquad \text{at } \bar{r}=1 \tag{20a}$$

or, for the general solution of Eq. (19), in terms of M, we have

$$\begin{aligned}\sum_{i=1}^{k}\Bigg\{&(a_0-1)\sum_{n=1}^{\infty}2e^{-b\tau}+\sum_{l=1}^{N}l!a_l\sum_{n=1}^{\infty}\frac{2(-1)^l}{b^l}\\&\times\left[e^{-b\tau}+\sum_{m=0}^{l-1}\frac{(-1)^{m+1}(b\tau)^m}{m!}\right]\\&+c_1\left[-e^{c_2\tau}+\sqrt{c_2}\coth(\sqrt{c_2})e^{c_2\tau}+\sum_{n=1}^{\infty}\frac{2\omega^2e^{-b\tau}}{(c_2+\omega^2)}\right]\\&+\frac{MR_2\bar{\sigma}T_i^3}{\alpha}\Theta^4\Bigg\}_i^2=0, \qquad \text{at } \bar{r}=1\end{aligned} \tag{20b}$$

where the summation is carried over the discretely measured k time steps. In Eq. (20), Θ^4 is known at each measurement from the experiment. The problem is now posed as a minimization problem, where the value of α that minimizes Φ gives the thermal diffusivity. Iordanov and Steward[14] describe a method to determine the thermal diffusivity in a solid slab. In their method, a function that minimizes the difference between the theoretically predicted and measured temperatures at an interior point is used. However, it is not possible in this case to measure temperature at an interior point. Hence, we minimize Eq. (20b), the function that satisfies heat balance at the surface. Using any suitable minimization method, Φ can be minimized. Here, a modified quasilinearization algorithm is used.

The experimental procedure to find α can be summarized as follows:

1) A small droplet (such that lumped analysis is valid) is levitated, heated to the desired temperature, and allowed to cool. The droplet size is measured, and the surface temperature history is recorded. Using Eq. (10), M is found.

2) The large-droplet experiment is conducted. A typical experiment lasts from 15 to 30 s. Due to the expected error in temperature measurements, as many data points as possible must be taken during the experiment. The surface temperature K is fitted against time (s) using a polynomial fit. Using the M from step 1, the functional Φ of Eq. (20b) is minimized. For each value of α during minimization, the temperature-time curve-fit constants are transformed to obtain the curve fit in the nondimensional (Θ-τ) domain. The minimizing α is the required thermal diffusivity.

Results and Discussion

The success of the experimental procedure outlined in the previous section depends upon ensuring that 1) the radius of the droplet is so chosen that lumped analysis is valid in the small-droplet experiment and Eq. (2) is valid in the large-droplet experiment, and 2) the assumptions of conduction within the sample and radiation outside are valid, i.e., convection or convective instabilities are absent within the droplet. We proceed now to examine whether these conditions are met and recognize any restrictions imposed.

Droplet Size

Using Eq. (8) and $Bi<0.1$ as the criterion, we can evaluate the droplet size requirements. Two extremes are of concern: as a result of the Biot number requirements, are the sample sizes in the large-droplet experiment too large, i.e., are they beyond the restriction imposed by a typical levitator, and are they too small in the small droplet experiment? Of the two, the first is the more alarming question, since restriction is on the largest possible size of the levitated sample. Table 1 lists the radius required for $Bi_r = 0.1$, for various commonly levitated metals. Although the diffusivity measurement technique is not limited to electromagnetic levitation of metals, it is only in metals, where k is usually high, that large sample sizes may result for the large-droplet experiment. It can be seen that for most metals, the radius required (for $Bi = 0.1$) is between 1 and 3 cm.

It must be remembered that the estimates in this analysis are conservative and are based on data at the highest available temperature in the solid phase.[1] Thermal conductivity usually decreases with temperature, and, in reality, will be lower than the value used in the calculations. Data indicate, where available, that there is a significant drop in thermal conductivity at the melting point. (It is not clear what happens beyond melting point, as very little data are available in this regime.) In addition, we have also assumed that the initial drop temperature (at the commencement of the cooling) is only 500 K greater than the melting point. In actual levitation experiments, one can heat several hundred degrees beyond the melting point. In fact, one way to reduce the large sample size (if necessary) is to increase the temperature levels of the experiment. Thus, the size requirements for successful thermal diffusivity measurements are well within physical reach for most materials of interest.

Other Modes of Heat Transfer Within the Droplet

As observed earlier, in the space environment, with near-zero gravity, natural buoyant convection is absent. However, a major concern, due to the transient nature of the problem, is Marangoni convection, especially since gravity is absent. The Marangoni number dictates onset of convective instability and is defined from the scaling analysis of the momentum equation (including the surface tension forces) as

$$Ma = -\left[\left(\frac{d\gamma}{dT}\Delta T\, a\right)\Big/\rho\right]\nu\kappa \tag{21}$$

Here, $d\gamma/dT$ is assumed to be constant. Usually, $d\gamma/dT = -10^{-4}$N/mK, and a is the characteristic size of the droplet (which we take here to be the radius).

To order of magnitude in SI units, $d\gamma/dT \approx 10^{-4}$, $\Delta T \approx 10^3$, $\rho \approx 10^3$, $\nu \approx 10^{-6}$, and $\kappa \approx 10^2$, resulting in

$$Ma \approx 10^{-2}a \tag{22}$$

From Patzer and Homsy,[15] the lowest critical Marangoni number for a droplet in cooling is found to be about 10. Using this in Eq. (22), we observe that the allowable diameters before Marangoni convection becomes significant are three orders of magnitude greater than those used in the experiments. Marangoni convection can, therefore, be safely neglected in the analysis.

Another concern if electromagnetic levitation is used is electromagnetic stirring within the droplet, which leads to forced convection. However, in space application, the electromagnetic forces are about three orders of magnitude lower than on earth. Moreover, the order of magnitude of fluid velocity is correspondingly smaller than the 0.1 m/s observed on earth. In actual experiments, once cooling begins, 3-4 s are given for the system to reach equilibrium before the actual data acquisition begins.

Demonstration of Procedure: Examples

Nickel, niobium, and palladium were chosen as examples to study the method described in the previous section. Two values of Nr ($Nr = 4$ and 10) were used. These values of Nr are the upper and lower limits of the values that may be used in actual experiments. The highest value of Nr that can be used is 10, since it corresponds to the smallest values of radius required, as Table 1 shows. At $Nr = 4$, the radius of the droplet is already too large to be accommodated in a levitator. Hence, these values were chosen in demonstrating this method. Table 2 lists the relevant properties used for the three materials.

In order to test the method, an experimental cooling curve is necessary for each material. However, no such experimental curves are available in the literature, to the best of the authors' knowledge. Therefore, the tests were conducted numerically using the theoretical curves obtained by Ayers,[16] for the transient cooling of a sphere exposed to a space environment. Since no liquid phase data were available, the tests were conducted in the solid phase, using available data from Touloukian et al.,[1] i.e., for an α value at a particular temperature, the surface temperature history was extracted for a given material from the theoretical results of Ayers.[15] The nondimensional cooling curves for a sphere cooling in space are depicted in Fig. 3. Linear, quadratic, cubic, and quartic curve fits were then used for each material. These curve fits were presented to the minimizing routine as "experimentally determined cooling curves," and the functional given by Eq. (20b) was minimized

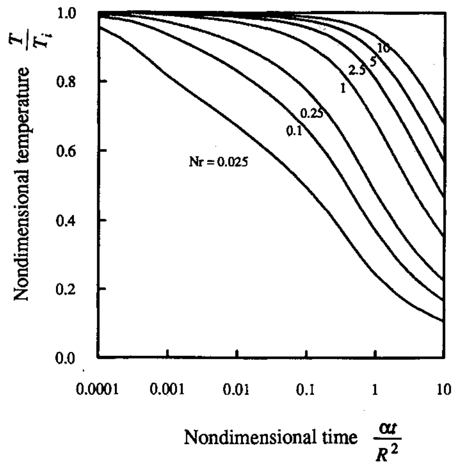

Fig. 3 Transient surface temperature of a sphere cooling in space.

Table 1 Size requirements for some liquid metals for diffusivity measurements[a]

Material	*mp* K	*bp* K	κ^b $Wm^{-1}K^{-1}$	*Bi*	$R(Bi = 0.1)$ m
Chromium	2118	2893	60 (1500)	6.8*r*	0.014
Cobalt	1765	3173	70 (600)	3.8*r*	0.026
Copper	1356	2843	131 (m.p.)	1.1*r*	0.11
Gold	1336	3223	250 (1000)	0.5*r*	0.2
Iron	1810	3343	30 (1600)	9.3*r*	0.01
Lead	600	2013	15 (m.p.)	2.0*r*	0.05
Molybdenum	2883	5823	80 (2000)	11*r*	0.009
Nickel	1726	3183	80 (1700)	3.1*r*	0.03
Niobium	2741	5200	80 (2200)	9.7*r*	0.01
Palladium	1825	3202	80 (1500)	3.6*r*	0.028
Tungsten	3653	5623	70 (m.p.)	23.2*r*	0.004
Vanadium	2192	3273	40 (m.p.)	11.1*r*	0.009

[a] Melting point and thermal conductivity data from Touloukian et al.[1] Boiling point data from Shimoji.[17] Biot number caluclations based on an initial sample temperature of $mp + 500$.

[b] Numbers in parentheses refer to the temperature at which κ values were taken.

Table 2 Relevant properties[a] **and parameters used in the verification**

Material	ρ Kg m^{-3}J	Cp Kg^{-1}K^{-1}	ϵ	*Nr*	T_{i2} K
Nickel	8495	607.0	0.3	4	1593.0
Niobium	7886.9	384.9	0.24	4	2113.0
Palladium	10800	316.9	0.2	10	1673.15

[a] Property data from Touloukian et al.[1]

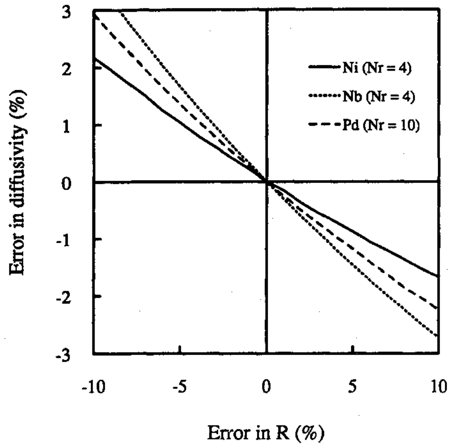

Fig. 4 Influence of error in R on diffusivity.

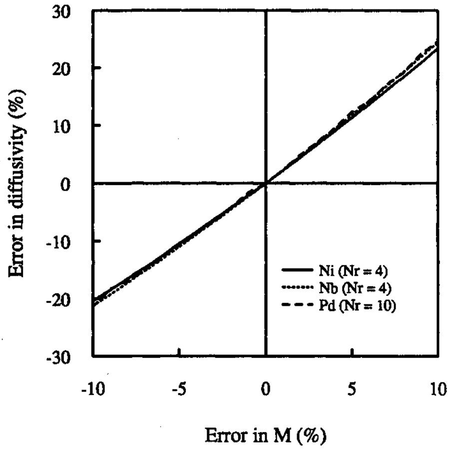

Fig. 5 Influence of error in M on diffusivity.

with respect to α using a modified quasilinearization algorithm. A FORTRAN program was developed that accepts material properties (Table 2) and the temperature history and determines the minimizing α for different degrees of the polynomial fit desired. The minimizing α was then compared to the expected α, and the error calculated. Table 3 lists the results for the three examples. The error is seen to reduce with better curve fits to the initial data. In fact, the reduction in error on proceeding to a higher-order curve fit is remarkable. In actual experiments, after neglecting the first 3-4 s (in order to account for initial transients, and allowing the system to come to equilibrium), the data must be fitted to the best possible fit before computing α.

Error Analysis

In order to qualify an experimental system, an error analysis, and a systematic study of error propagation are essential. In this section, we present the results of a numerical error-study when the best fit (quartic) is used. The specific error sources studied are 1) error in the initial data and curve fitting, 2) error in the measurement of radius, and 3) error in the M value obtained from the first experiment.

Before actually studying the error propagation due to errors in these parameters, the effect of changing the degree of curve fit on error propagation was also studied. Such a study is important, since the terms included in Eq. (20b) change for different degrees of curve fit. It was found that there is little or no effect (less than 0.5%) of varying the fit on the error in α. Thus, using higher-order fits does not influence the error propagation adversely or otherwise. However, this may not be true in the case of actual experimental data, where the error may be significant. It is therefore advisable to run a similar error analysis on any experimental data-set before deciding upon the curve fits to be employed.

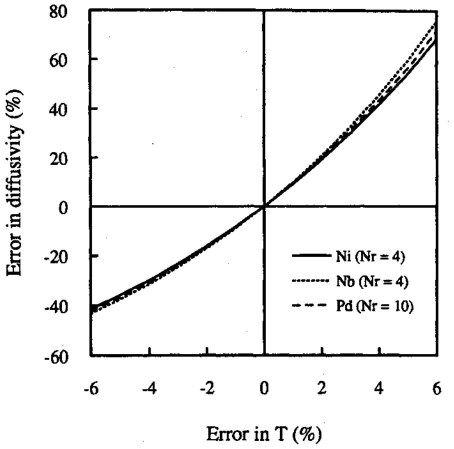

Fig. 6 Influence of error in T on diffusivity.

Table 3 Thermal diffusivity determination: error for various fits

		Percentage error in α			
Material	$\alpha \times 10^{-5}$ m^2s^{-1}	linear	quadr.	cubic	quartic
Nickel ($Nr = 4$)	1.60	9.26	5.77	2.37	1.38
Niobium ($Nr = 4$)	2.84	11.78	14.60	4.90	0.868
Palladium ($Nr = 10$)	3.14	9.19	7.27	3.04	1.43

In actual experiments, the radius is measured from high-resolution high-speed photographs of the droplet. Figure 4 depicts the effect of an error in radius on the value of α. The error in radius does not have a significant influence on α. For example, in the worst case, for 1-2% error expected in the radius measurements, the corresponding error in α is only about 0.5%. Thus, errors in radius measurements do not adversely affect α determination.

Figure 5 shows the influence of error in the measurement of M on the error in diffusivity for all three materials. In the experiments, M is found from measurements performed in the first (small-droplet) study and will always have an inherent error. A simple error analysis of Eq. (10) leads to the error equation for M,

$$(\delta M\,\%) = [(\delta R\,\%)^2 + (\delta t\,\%)^2 + 3(\delta T\,\%)^2 + 3(\delta T_{i1}\,\%)^2]^{1/2} \quad (23)$$

In Eq. (24), the error in t measurements, which is very small, can be neglected. The error in R is of the order of 0.5-1%. Thus, the error in M is strongly influenced by the error in measuring T in the first experiment. For example, for a 1.5% error in T (about 30 K) in the first experiment, the corresponding error in M is about 3.6%, which leads, from Fig. 5, to an error of about 6–7% in α. Thus, this is the lower limit of error in this method. This error is better than the error introduced when the available values of ρ, C_p, and ϵ at these high temperatures are directly used. The error may be reduced by improving the measurement of the small-droplet experimental parameters.

The most important influence on the error in α is the error in temperature. Figure 6 depicts the behavior of error in α with error in temperature measurements. As can be seen, the effect of error in measurement of temperature in the second (large-drop) experiment on the error in α is drastic. Therefore, a very accurate temperature measurement method may be necessary to get accurate α results.

Conclusions

A method to determine the thermal diffusivity of materials at high temperatures has been presented. The method is applied in two parts—a small-droplet and a large-droplet experiment—in order to eliminate the need to know the density, specific heat, and emissivity of the materials being studied. An inverse conduction problem is formulated for the large-droplet case and solved using Laplace transformation techniques. The extra boundary condition (the heat balance at the boundary) is posed as a function to be minimized, and the α that minimizes it is found using the modified quasilinearization algorithm. The solution method is demonstrated for three materials and two conduction-to-radiation parameters, which are typical of the envisaged experiments. This method is shown to be accurate within 2% for good curve fits of initial data. Error analysis shows that the error in temperature and M measurement affects the accuracy of measurement of α significantly.

The above method has to be verified via actual experiments. Undoubtedly, direct experimentation in space or reduced gravity environments is expensive. Therefore, Earth-based experimentation on solid spherical objects is recommended. Such experiments may be easily performed using radiatively heating furnaces and evacuated chambers with cold isothermal walls. Once this is accomplished, the real thrust of this method, the measurement of thermal diffusivity of liquids at elevated temperatures, may be realized.

References

[1]Touloukian, Y. S., Powell, R. W., Ho, C. Y., and Nicolaou, M. C., *Thermophysical Properties of Matter*, IFI/Plenum, New York-Washington, 1973.

[2]Nieto de Castro, C. A., Taxis, B., Roder, H. M., and Wakeham, W. A., "Thermal Diffusivity Measurements by the Transient Hot-Wire Technique: A Reappraisal," *International Journal of Thermophysics*, Vol. 9, May 1988, pp. 293–316.

[3]Alloush, A., Gosney, W. B., and Wakeham, W. A., "A Transient Hot-Wire Instrument for Thermal Conductivity Measurements in Electrically Conducting Liquids at Elevated Temperatures," *International Journal of Thermophysics*, Vol. 3, March 1982, pp. 225–235.

[4]Schriempf, J. T., "A Laser Flash Technique for Determining Thermal Diffusivity of Liquid Metals at Elevated Temperatures," *Review of Scientific Instruments*, Vol. 43, May 1972, pp. 781.

[5]Cezairliyan, A., "A Dynamic Technique for Measurements of Thermophysical Properties at High Temperatures," *International Journal of Thermophysics*, Vol. 5, 1984, pp. 177–193.

[6]Araki, N., "Measurements of Thermophysical Properties by a Stepwise Heating Method," *International Journal of Thermophysics*, Vol. 5, 1984, pp. 53–71.

[7]Araki, N., and Natsui, K., "Measuring Thermal Diffusivity of Liquids by Stepwise Heating, The First Report, Principle Measuring, Method and Theoretical Analysis of Errors," *Transactions Japanese Society Mechanical Engineers*, Vol. 49, Pt. B, 1983, pp. 1048–1057.

[8]Beck, J. V., Blackwell, B., and St. Clair, C., Jr., *Inverse Heat Conduction-Ill-Posed Problems*, Wiley-Interscience, New York, 1985.

[9]Barmatz, M., "Overview of Containerless Processing Technologies," *Materials Processing in the Reduced Gravity Environment of Space*, edited by G. E., Rindone, North Holland, Amsterdam, 1982, pp. 25–37.

[10]Hansen, G. P., Krishnan, S., Hauge, R. H., and Margrave, J. L., "Measurement of Temperature and Emissivity of Specularly Reflecting Glowing Bodies," *Metallurgical Transactions A*, Vol. 19A, Aug. 1988, pp. 1889–1894.

[11]Bayazitoglu, Y., and Suryanarayana, P. V. R., "Transient Cooling of a Sphere Surrounded by a Participating Medium," *Proceedings of the ASME Winter Annual Meeting*, Vol. 104, American Society of Mechanical Engineers, New York, 1988, pp. 31–35.

[12]Bayazitoglu, Y., and Suryanarayana, P. V. R., "Transient Radiative Heat Transfer from a Sphere Surrounded by a Participating Medium," *Journal of Heat Transfer*, Vol. 111, 1990, pp. 713–717.

[13]Ho, C. Y., (ed.), *CINDAS Data Series on Material Properties*, Vol. I-2, Hemisphere, New York, 1986.

[14]Iordanov, V. I., and Steward, A. P., "A Method and a Computer Program for Determining the Thermal Diffusivity in a Solid Slab," *Applied Mathematical Modelling*, Vol. 8, 1984, pp. 169–178.

[15]Patzer, J. F., and Homsy, G. H., "Global Stability of Transient Drop Extraction to Marangoni Instabilities," *Physics of Fluids*, Vol. 24, April 1981, pp. 567–575.

[16]Ayers, D. L., "Transient Cooling of a Sphere in Space," *Journal of Heat Transfer*, Vol. 92, Ser. C., 1970, pp. 180–182.

[17]Shimoji, M., *Liquid Metals*, Academic, London, 1977.